

Survival probability of charged particles dissipating their energies by radiation and ionization

Atsushi Iyono*

Department of Fundamental Science, Okayama University of Science, Okayama 700-0005, Japan

E-mail: iyono@das.ous.ac.jp

S. Yamamoto

Department of Fundamental Science, Okayama University of Science, Okayama 700-0005, Japan

S. Tsuji, K. Okei, H. Matsumoto

Department of Natural Sciences, Kawasaki Medical School, Kurashiki 701-0192, Japan

T. Nakatsuka

Laboratory of Information Science, Okayama Shoka University, Okayama 700-8601, Japan

The survival probabilities of charged particle traversing through matters are evaluated by solving the diffusion equation, taking account of radiation and ionization losses. The solutions corresponding to high and low incident energies are proposed respectively, and inaccuracies of the saddle point method appearing in case of large probabilities are removed by deriving the results via the complementary probabilities. The enough-accurate results will be valuable to improve the resolution of radiographic analyses with atmospheric muons, and others.

35th International Cosmic Ray Conference — ICRC2017

10–20 July, 2017

Bexco, Busan, Korea

*Speaker.

1. Introduction

The radiographic analyses with atmospheric muons are applied to the inner-structure investigations of various objects, e.g. geophysical substances like volcanic mountains [1, 2], large-volume rock structure like pyramids [3, 4], inaccessible cores of the damaged nuclear reactors [5], and others. Precise evaluations of transmission efficiency for penetrating muons are important for these radiographic methods. Many Monte Carlo simulations are performed to clarify the process [2, 5, 6]. We evaluate transmission efficiency analytically by solving the diffusion equation for penetrating charged particles, taking account of radiation and ionization losses. The results are compared with those derived by our simple Monte Carlo simulations.

2. The diffusion equation for energy dissipation of charged particles

Charged particles dissipate their energies by radiation and ionization when they traverse through matters. The diffusion equation for the differential energy spectrum $\pi(E_0, E, t)$ of charged particles is described as

$$\frac{\partial}{\partial t} \pi(E_0, E, t) = - \int_0^1 \left\{ \pi(E_0, E, t) - \frac{1}{1-v} \pi(E_0, \frac{E}{1-v}, t) \right\} \phi(v) dv + \varepsilon \frac{\partial}{\partial E} \pi(E_0, E, t), \quad (2.1)$$

where t denotes the traversed thickness measured in radiation unit, $\phi(v)dv$ the probability of fractional energy loss, and ε the constant energy loss in unit radiation length [7]. If we express

$$\pi(E_0, E, t) dE = \frac{dE}{(2\pi i)^2} \iint \frac{ds}{E} \left(\frac{E_0}{E} \right)^s \Gamma(-q) \left(\frac{\varepsilon}{E} \right)^q \mathcal{M}(s, q, t) dq \quad (2.2)$$

by introducing M-function of $\mathcal{M}(s, q, t)$ [8], the diffusion equation (2.1) is expressed as

$$\left\{ \frac{\partial}{\partial t} + A(s+q) \right\} \mathcal{M}(s, q, t) = (s+q)q \mathcal{M}(s, q-1, t) \quad \text{with} \quad \mathcal{M}(s, 0, 0) = 1, \quad (2.3)$$

where $A(s)$ denotes the characteristic energy-dissipating function derived by

$$A(s) \equiv \int_0^1 \{1 - (1-v)^s\} \phi(v) dv. \quad (2.4)$$

We apply $A(s)$ of electron indicated in Rossi and Greisen [7] in this report.

3. The survival probabilities under Approx. A

3.1 The results ordinarily derived by the saddle point method

The differential energy spectrum $\pi(E_0, E, t)$ with $\varepsilon = 0$ (Approx. A) is derived as the residue at $q = 0$ of Eq. (2.2), so that we have

$$\mathcal{M}(s, 0, 0) = e^{-A(s)t} \quad \text{and} \quad (3.1)$$

$$\pi(E_0, E, t) dE = \frac{dE}{2\pi i} \int \frac{ds}{E} \left(\frac{E_0}{E} \right)^s e^{-A(s)t}. \quad (3.2)$$

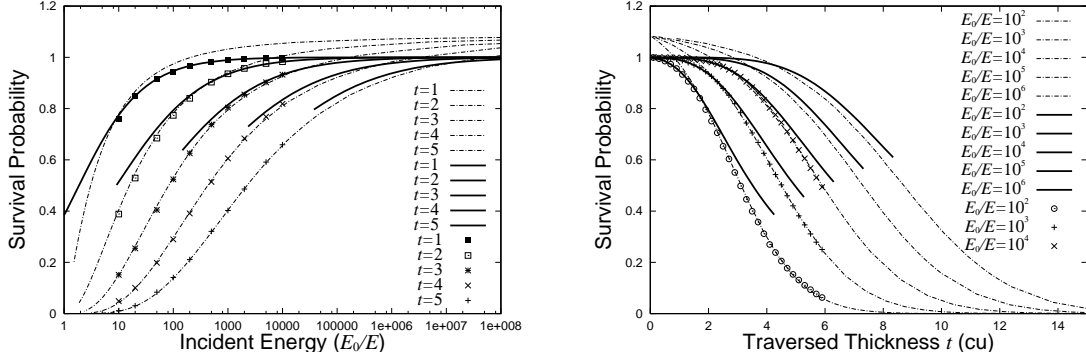


Figure 1: Survival probabilities with $\varepsilon = 0$ (Approx. A) versus E_0/E at $t = 1, 2, 3, 4, 5$ (left panel) and those versus t with $E_0/E = 10^2, 10^3, 10^4, 10^5, 10^6$ (right panel), derived by the ordinary transform (thin lines), via complementary probabilities (thick lines), and by Monte Carlo simulations (dots).

Then the survival probability $\pi(E_0, > E, t)$ of charged particles with their energies greater than E is obtained as

$$\pi(E_0, > E, t) \equiv \int_E^\infty \pi(E_0, E, t) dE = \frac{1}{2\pi i} \int \frac{ds}{s} \left(\frac{E_0}{E} \right)^s e^{-A(s)t}, \quad (3.3)$$

where the path of integration is taken at $0 < \mathcal{R}(s)$. We can evaluate the probability ordinarily by the saddle point method,

$$\pi(E_0, > E, t) \simeq (E_0/E)^{\bar{s}} e^{-A(\bar{s})t} / \sqrt{2\pi\{1 - \bar{s}^2 A''(\bar{s})t\}}, \quad \text{with} \quad (3.4)$$

$$\ln(E_0/E) \simeq A'(\bar{s})t + 1/\bar{s} \quad \text{and} \quad 0 < \bar{s}. \quad (3.5)$$

The survival probabilities versus E_0/E so obtained at $t = 1, 2, 3, 4,$ and 5 are indicated in the left panel of Fig. 1 (dot lines, from left to right). Also, those versus t with $E_0/E = 10^2, 10^3, 10^4, 10^5,$ and 10^6 are indicated in the right panel of Fig. 1 (dot lines, from left to right).

3.2 The results derived via the complementary probability

The ordinary results of the survival probability derived above by the saddle point method show ill accuracy at the large-probability region [9], giving the limiting value of $e/\sqrt{2\pi} \simeq 1.08$ to $\pi(E_0, > E, t)$ at $E_0/E \rightarrow \infty$ in the left panel and at $t \rightarrow 0$ in the right panel of Fig. 1, respectively. To avoid this inaccuracy, we introduce the complementary probability $\pi^*(E_0, > E, t)$ defined by

$$\pi^*(E_0, > E, t) \equiv -\frac{1}{2\pi i} \int \frac{ds}{s} \left(\frac{E_0}{E} \right)^s e^{-A(s)t}, \quad (3.6)$$

where we moved the path of integration to $-1 < \mathcal{R}(s) < 0$. The residue of 1 at $s = 0$ causes the complementary relation of

$$\pi(E_0, > E, t) + \pi^*(E_0, > E, t) = 1, \quad (3.7)$$

so that the survival probability can also be evaluated by the saddle point method as

$$\pi(E_0, > E, t) \simeq 1 - (E_0/E)^{\bar{s}} e^{-A(\bar{s})t} / \sqrt{2\pi\{1 - \bar{s}^2 A''(\bar{s})t\}}, \quad \text{with} \quad (3.8)$$

$$\ln(E_0/E) \simeq A'(\bar{s})t + 1/\bar{s} \quad \text{and} \quad -1 < \bar{s} < 0. \quad (3.9)$$

The results are indicated in the left and the right panels of Fig. 1 (thick solid lines), which give the exact limiting values of 1 at $E_0/E \rightarrow \infty$ and at $t \rightarrow 0$.

To examine accuracies of the result, we carried out a Monte Carlo simulation of cascade showers [10] and investigated the survival probabilities of the incident electron (dots), and we have confirmed that the ordinary results of survival probability and the results via the complementary probability show good accuracies in the low- and the high-probability regions, respectively.

4. The survival probabilities under Approx. B

4.1 Solution of the survival probabilities

The diffusion equation (2.3), taking account of both radiation and ionization losses (Approx. B), can be expressed as

$$\{\lambda + A(s+q)\} \mathcal{L}(s, q, \lambda) = (s+q)q \mathcal{L}(s, q-1, \lambda) + \delta_{q,0} \quad (4.1)$$

by applying Laplace transform to $\mathcal{M}(s, q, t)$,

$$\mathcal{L}(s, q, \lambda) = \int_0^\infty e^{-\lambda t} \mathcal{M}(s, q, t) dt, \quad (4.2)$$

according to Nishimura [8]. Then we have

$$\mathcal{L}(s, q, \lambda) = \frac{\Gamma(s+q+1)\Gamma(q+1)}{\Gamma(s+1)} \frac{1}{\lambda + A(s)} \lim_{m \rightarrow \infty} \{\lambda + A(s+m+1)\}^{-q} \prod_{j=1}^m \frac{\lambda + A(s+q+j)}{\lambda + A(s+j)}, \quad (4.3)$$

thus the survival probability $\pi(E_0, E > 0, t)$ of charged particles at t is derived by integrating (2.2) from E to infinity and taking the limiting value at $E \rightarrow 0$, as

$$\begin{aligned} \pi(E_0, E > 0, t) &\equiv \frac{1}{2\pi i} \int \left(\frac{E_0}{\varepsilon}\right)^s \Gamma(s) \mathcal{M}(s, -s, t) ds \\ &= \frac{1}{(2\pi i)^2} \iint \left(\frac{E_0}{\varepsilon}\right)^s e^{t\lambda} \Gamma(s) \mathcal{L}(s, -s, \lambda) ds d\lambda. \end{aligned} \quad (4.4)$$

4.2 The solution in case of large E_0/ε

The survival probability $\pi(E_0, E > 0, t)$ expressed in (4.4) can be evaluated as

$$\pi(E_0, E > 0, t) \simeq (E_0/\varepsilon)^{\bar{s}} \Gamma(\bar{s}) \mathcal{M}(\bar{s}, -\bar{s}, t) / \sqrt{2\pi(\partial^2/\partial s^2) \ln \{\Gamma(\bar{s}) \mathcal{M}(\bar{s}, -\bar{s}, t)\}}, \quad \text{with} \quad (4.5)$$

$$\ln(E_0/\varepsilon) + (\partial/\partial s) \ln \{\Gamma(\bar{s}) \mathcal{M}(\bar{s}, -\bar{s}, t)\} = 0 \quad \text{and} \quad 0 < \bar{s} \quad (4.6)$$

by applying the saddle point method ordinarily, where $\Gamma(s)\mathcal{M}(s, -s, t)$ is expressed as

$$\Gamma(s)\mathcal{M}(s, -s, t) = \sum_{k=0}^{\infty} \Gamma(s)\mathcal{M}_k(s, -s) e^{-A(s+k)t} \quad \text{with} \quad (4.7)$$

$$\Gamma(s)\mathcal{M}_0(s, -s) = -\Gamma(-s) \lim_{m \rightarrow \infty} \{A(s+m+1) - A(s)\}^s \prod_{j=1}^m \frac{A(j) - A(s)}{A(s+j) - A(s)} \quad \text{and} \quad (4.8)$$

$$\Gamma(s)\mathcal{M}_k(s, -s) = -\Gamma(-s) \frac{A(k) - A(s+k)}{A(s) - A(s+k)} \times \lim_{m \rightarrow \infty} \{A(s+m+1) - A(s+k)\}^s \prod_{j=1, j \neq k}^m \frac{A(j) - A(s+k)}{A(s+j) - A(s+k)} \quad (4.9)$$

as indicated ever [8, 11]. Derivatives of $\Gamma(s)\mathcal{M}(s, -s, t)$ are expressed as

$$\frac{\partial}{\partial s} \{\Gamma(s)\mathcal{M}(s, -s, t)\} = \sum_{k=0}^{\infty} \left[\frac{\partial}{\partial s} \{\Gamma(s)\mathcal{M}_k(s, -s)\} - A'(s+k)t \{\Gamma(s)\mathcal{M}_k(s, -s)\} \right] e^{-A(s+k)t}, \quad (4.10)$$

$$\frac{\partial^2}{\partial s^2} \{\Gamma(s)\mathcal{M}(s, -s, t)\} = \sum_{k=0}^{\infty} \left[\frac{\partial^2}{\partial s^2} \{\Gamma(s)\mathcal{M}_k(s, -s)\} - 2A'(s+k)t \frac{\partial}{\partial s} \{\Gamma(s)\mathcal{M}_k(s, -s)\} + \{A'(s+k)^2 t^2 - A''(s+k)t\} \{\Gamma(s)\mathcal{M}_k(s, -s)\} \right] e^{-A(s+k)t}. \quad (4.11)$$

The survival probabilities versus E_0/ε so obtained at $t = 1, 2, 3, 4,$ and 5 are indicated in the right panel of Fig. 2 (dot lines, from top to bottom). Summation (4.7) was taken up to k of 10. Derivatives of $\Gamma(s)\mathcal{M}_k(s, -s)$ are evaluated numerically. This method is valid at $10 \lesssim E_0/\varepsilon$, due to the convergence. We compared the results with the survival probabilities of incident electron certified in the Monte Carlo simulation. Both results agree well at the relatively low-probability region.

Discrepancies at the high-probability region come from the inaccuracy of the saddle point method in this region. We introduce the complementary probability of

$$\pi^*(E_0, E > 0, t) \equiv -\frac{1}{2\pi i} \int \left(\frac{E_0}{\varepsilon}\right)^s \Gamma(s)\mathcal{M}(s, -s, t) ds \simeq (E_0/\varepsilon)^{\bar{s}} \Gamma(\bar{s})\mathcal{M}(\bar{s}, -\bar{s}, t) / \sqrt{2\pi(\partial^2/\partial s^2) \ln \{\Gamma(\bar{s})\mathcal{M}(\bar{s}, -\bar{s}, t)\}}, \quad \text{with} \quad (4.12)$$

$$\ln(E_0/\varepsilon) + (\partial/\partial s) \ln \{\Gamma(\bar{s})\mathcal{M}(\bar{s}, -\bar{s}, t)\} = 0 \quad \text{and} \quad -1 < \bar{s} < 0, \quad (4.13)$$

then $\pi(E_0, E > 0, t)$ obtained through the relation of (3.7) show good agreement with the Monte Carlo results, as indicated in the figure. Note that $\pi^*(E_0, E > 0, t)$ defined here can be applied to obtain the probability for smaller E_0/ε regions (up to $2 \lesssim E_0/\varepsilon$), as indicated in the left panel of the figure.

Also, the survival probabilities versus t with $E_0/\varepsilon = 10, 10^2, 10^3, 10^4, 10^5,$ and 10^6 are indicated in the right panel of Fig. 3 (dot lines, from left to right). In this case, it requires much iteration works to find \bar{s} or t corresponding to E_0/ε in Eq. (4.6). Fortunately, we can well approximate the summation (4.7) by the first term ($k = 0$). Then we can effectively determine t by

$$A'(\bar{s})t = \ln(E_0/\varepsilon) + (\partial/\partial s) \ln \{\Gamma(\bar{s})\mathcal{M}_0(\bar{s}, -\bar{s})\}. \quad (4.14)$$

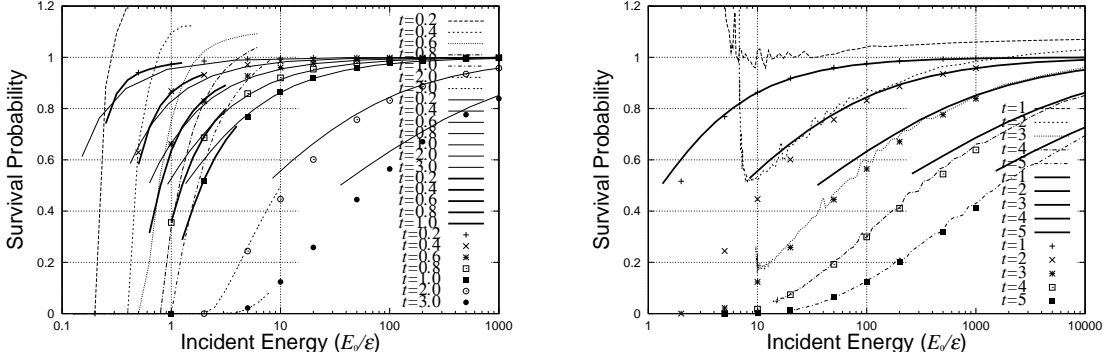


Figure 2: Survival probabilities (Approx. B) versus E_0/ε at $t = 0.2, 0.4, 0.6, 0.8, 1, 2, 3$ (left panel) and those at $t = 1, 2, 3, 4, 5$ (right panel), derived by the ordinary transform (thin dot lines), via complementary probabilities (thick lines), via the extended complementary probabilities from large E_0/ε region (thin lines in the left panel), and by Monte Carlo simulations (dots).

This method is valid at $10 \lesssim E_0/\varepsilon$, due to the convergence. The results also agree well with the Monte Carlo results (dots) at the relatively low-probability region. At the high-probability region, we obtain the survival probabilities via the complementary probability of (4.12) with (4.14) and $-1 < \bar{s} < 0$. The results agree well with the Monte Carlo results (dots), as indicated in the figure.

4.3 The solution in case of small E_0/ε

In case of $E_0/\varepsilon \ll 1$, $\pi(E_0, E > 0, t)$ indicated in the last subsection diverges, so that we evaluate the survival probability of (4.4) as

$$\begin{aligned} \pi(E_0, E > 0, t) &= \frac{1}{2\pi i} \int e^{t\lambda} \Sigma(E_0/\varepsilon, \lambda) d\lambda \\ &\simeq e^{t\bar{\lambda}} \Sigma(E_0/\varepsilon, \bar{\lambda}) / \sqrt{2\pi(\partial^2/\partial\lambda^2)\{\ln\Sigma(E_0/\varepsilon, \bar{\lambda})\}}, \quad \text{with} \quad (4.15) \\ t &\simeq -(\partial/\partial\lambda)\{\ln\Sigma(E_0/\varepsilon, \bar{\lambda})\} \quad \text{and} \quad -\infty < \bar{\lambda} < \infty, \quad (4.16) \end{aligned}$$

where we introduce $\Sigma(E_0/\varepsilon, \lambda)$ as

$$\begin{aligned} \Sigma(E_0/\varepsilon, \lambda) &= \frac{1}{2\pi i} \int \left(\frac{E_0}{\varepsilon}\right)^s \Gamma(s) \mathcal{L}(s, -s, \lambda) ds \\ &= -\frac{1}{2\pi i} \int ds \left(\frac{E_0}{\varepsilon}\right)^s \frac{\Gamma(-s)}{\lambda + A(s)} \lim_{m \rightarrow \infty} \{\lambda + A(s+m+1)\}^s \prod_{j=1}^m \frac{\lambda + A(j)}{\lambda + A(s+j)}, \quad (4.17) \end{aligned}$$

with the path of integration taken at $0 < \Re(s) < 1$. As $\Gamma(-s)$ gives the residue of $-(-1)^k/k!$ at $s = k$, we have

$$\begin{aligned} \Sigma(E_0/\varepsilon, \lambda) &= -\sum_{k=1}^{\infty} \frac{1}{k!} \left(-\frac{E_0}{\varepsilon}\right)^k \frac{1}{\lambda + A(k)} \lim_{m \rightarrow \infty} \{\lambda + A(k+m+1)\}^k \prod_{j=1}^m \frac{\lambda + A(j)}{\lambda + A(k+j)} \\ &= -\sum_{k=1}^{\infty} \frac{1}{k!} \left(-\frac{E_0}{\varepsilon}\right)^k \frac{1}{\lambda + A(k)} \prod_{j=1}^k (\lambda + A(j)). \quad (4.18) \end{aligned}$$

Note that the denominator of $\lambda + A(k)$ is cancelled by the last factor in the product, in this formula. And the derivatives of $\Sigma(E_0/\varepsilon, \lambda)$ are expressed as

$$\frac{\partial}{\partial \lambda} \Sigma(E_0/\varepsilon, \lambda) = - \sum_{k=2}^{\infty} \frac{1}{k!} \left(-\frac{E_0}{\varepsilon} \right)^{k-1} \prod_{j=1}^{k-1} (\lambda + A(j)) \sum_{j=1}^{k-1} \frac{1}{\lambda + A(j)}, \quad (4.19)$$

$$\frac{\partial^2}{\partial \lambda^2} \Sigma(E_0/\varepsilon, \lambda) = - \sum_{k=3}^{\infty} \frac{2}{k!} \left(-\frac{E_0}{\varepsilon} \right)^{k-1} \prod_{j=1}^{k-1} (\lambda + A(j)) \sum_{j=1}^{k-2} \frac{1}{\lambda + A(j)} \sum_{m=j+1}^{k-1} \frac{1}{\lambda + A(m)}. \quad (4.20)$$

The survival probabilities versus E_0/ε so obtained at $t = 0.2, 0.4, 0.6, 0.8, 1, 2,$ and 3 are indicated in the left panel of Fig. 2 (dot lines, from left to right). This method is valid at $E_0/\varepsilon \lesssim 10$. The results agree well with the Monte Carlo results (dots) at the relatively low-probability region.

At the high-probability region, we introduce the complementary probability

$$\begin{aligned} \pi^*(E_0, E > 0, t) &\equiv \frac{1}{2\pi i} \int e^{t\lambda} \Sigma^*(E_0/\varepsilon, \lambda) d\lambda \\ &\simeq e^{t\bar{\lambda}} \Sigma^*(E_0/\varepsilon, \bar{\lambda}) / \sqrt{2\pi(\partial^2/\partial \lambda^2)\{\ln \Sigma^*(E_0/\varepsilon, \bar{\lambda})\}}, \quad \text{with} \quad (4.21) \\ t &\simeq -(\partial/\partial \lambda)\{\ln \Sigma^*(E_0/\varepsilon, \bar{\lambda})\} \quad \text{and} \quad 0 < \bar{\lambda}, \quad (4.22) \end{aligned}$$

where

$$\Sigma^*(E_0/\varepsilon, \lambda) \equiv -\frac{1}{2\pi i} \int \left(\frac{E_0}{\varepsilon} \right)^s \Gamma(s) \mathcal{L}(s, -s, \lambda) ds = 1/\lambda - \Sigma(E_0/\varepsilon, \lambda). \quad (4.23)$$

Note that the residue of $1/\lambda$ at $s = 0$ was taken into account as the path of integration was moved to $\Re(s) < 0$. And we have

$$(\partial/\partial \lambda) \Sigma^*(E_0/\varepsilon, \lambda) = -1/\lambda^2 - (\partial/\partial \lambda) \Sigma(E_0/\varepsilon, \lambda), \quad (4.24)$$

$$(\partial^2/\partial \lambda^2) \Sigma^*(E_0/\varepsilon, \lambda) = 2/\lambda^3 - (\partial^2/\partial \lambda^2) \Sigma(E_0/\varepsilon, \lambda). \quad (4.25)$$

The survival probability obtained here from $\pi^*(E_0, E > 0, t)$ through the relation of (3.7) well interpolate that from (4.12) and that of (4.15) and explain the Monte Carlo results (dots) at the high-probability region, as indicated in the figure (thick solid lines).

Also, the survival probabilities versus t with $E_0/\varepsilon = 0.1, 0.2, 0.5, 1.0,$ and 2.0 are indicated in the left panel of Fig. 3 (dot lines, from left to right). The results also agree well with the Monte Carlo results (dots) at the relatively low-probability region, on the contrary the complementary probability (4.21) with (4.22) defined above well explains the Monte Carlo results through the relation of (3.7), as indicated in the figure (thick solid lines). This method is valid at $E_0/\varepsilon \lesssim 2$. Note that the curves in the left panel with $2 < E_0/\varepsilon < 10$ can be derived by applying the complementary probability (4.12) defined in the preceding subsection.

5. Conclusions and discussions

Transmission efficiencies of charged particle traversing through matter are investigated analytically, by solving the diffusion equation taking account of radiation and ionization losses. The solutions corresponding to high and low incident energies are proposed respectively, due to the

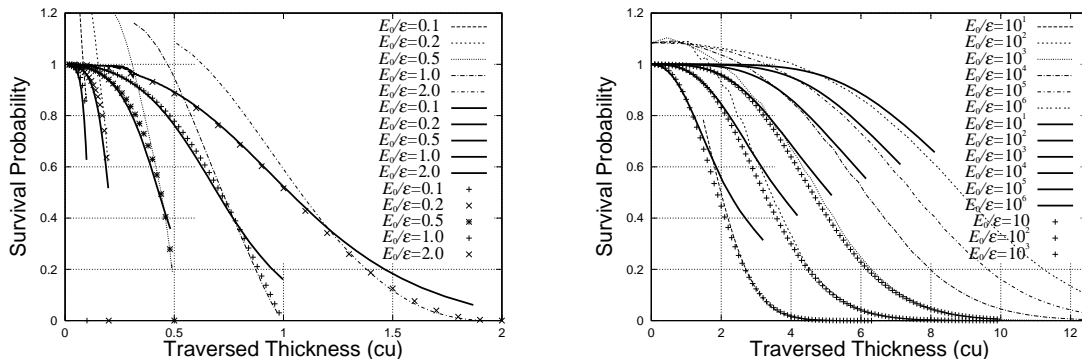


Figure 3: Survival probabilities (Approx. B) versus t with $E_0/\epsilon = 0.1, 0.2, 0.5, 1.0, 2.0$ (left panel) and those with $E_0/\epsilon = 10, 10^2, 10^3, 10^4, 10^5, 10^6$ (right panel), derived by the ordinary transform (thin lines), via complementary probabilities (thick lines), and by Monte Carlo simulations (dots).

difference of convergence condition. Well-known inaccuracies of the saddle point method appearing at the high-probability regions are removed by the derivation introducing the complementary probability. Highly accurate results of the transmission efficiency acquired without fluctuations will improve the resolution of radiographic analyses.

Acknowledgments

The authors are very indebted to Prof. Jun Nishimura for valuable advices and encouragements.

References

- [1] K. Nagamine, et al., Nucl. Instr. and Meth. A 356(1995)585.
- [2] H.K.M. Tanaka, et al., Nucl. Instr. and Meth. A 575(2007)489.
- [3] L.W. Alvarez, et al., Science 167(1970)832.
- [4] S.S. Patel, Archaeology, 61(2008)30.
- [5] K. Borozdin, et al., Phys. Rev. Lett. 109(2012)152501.
- [6] H.K.M. Tanaka, et al., Geophysical Research Letter, 36(2009)L01304.
- [7] B. Rossi and K. Greisen, Rev. Mod. Phys. 27(1941)240.
- [8] J. Nishimura, in *Handbuch der Physik, Band 46*, edited by S. Flügge (Springer, Berlin, 1967), Teil 2, p. 1.
- [9] L. Eyges, Phys. Rev., 76(1949)264.
- [10] T. Nakatsuka, Proc. 18th ICRC, Bangalore, 11(1983)299.
- [11] K. Kobayakawa, Nuovo Cim., B47(1967)156.